



**HAL**  
open science

## Modal Dependence of Rayleigh Scattering Coefficients Based on the Bidirectional OTDR Technique

Maroun Bsaibes, Yves Quiquempois, Marianne Bigot, H el ene Maerten, Pierre Sillard, Maxime Droques, Masaaki Hirano, Laurent Bigot

► **To cite this version:**

Maroun Bsaibes, Yves Quiquempois, Marianne Bigot, H el ene Maerten, Pierre Sillard, et al.. Modal Dependence of Rayleigh Scattering Coefficients Based on the Bidirectional OTDR Technique. Optics and Lasers in Engineering, 2023, 171, 10.1016/j.optlaseng.2023.107795 . hal-04245456

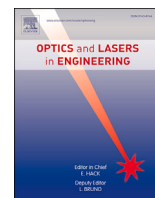
**HAL Id: hal-04245456**

**<https://hal.science/hal-04245456>**

Submitted on 19 Nov 2023

**HAL** is a multi-disciplinary open access archive for the deposit and dissemination of scientific research documents, whether they are published or not. The documents may come from teaching and research institutions in France or abroad, or from public or private research centers.

L'archive ouverte pluridisciplinaire **HAL**, est destin ee au d ep ot et  a la diffusion de documents scientifiques de niveau recherche, publi es ou non,  emanant des  tablissements d'enseignement et de recherche franais ou  trangers, des laboratoires publics ou priv es.



# Modal dependence of Rayleigh scattering coefficients based on the bidirectional OTDR technique

Maroun Bsaibes<sup>a,\*</sup>, Yves Quiquempois<sup>a</sup>, Marianne Bigot<sup>b</sup>, H el ene Maerten<sup>b</sup>, Pierre Sillard<sup>b</sup>, Maxime Droques<sup>c</sup>, Masaaki Hirano<sup>d</sup>, Laurent Bigot<sup>a</sup>

<sup>a</sup> Univ. Lille, CNRS, UMR 8523 – PhLAM – Physique des Lasers, Atomes et Mol cules, 2 Av. Jean Perrin, Lille, 59000, Hauts-de-france, France

<sup>b</sup> Prysmian Group, Parc des Industries Artois Flandres, Haisnes Cedex, 62092, Hauts-de-france, France

<sup>c</sup> Alcatel Submarine Networks, 950, Quai de la Loire, Calais Cedex, 62225, Hauts-de-france, France

<sup>d</sup> Sumitomo Electric Industries, Ltd., 1, Taya-cho, Sakae-ku, Yokohama, 244-8588, Kanto, Japan

## ARTICLE INFO

### Keywords:

Rayleigh scattering  
Attenuation  
OTDR  
Few-mode fiber

## ABSTRACT

In this work, a simple method based on optical time-domain reflectometry has been implemented to compare the Rayleigh scattering coefficient of different modes of few-mode fibers. The principle of the method is first validated in the case of single-mode fibers and then applied to two weakly-coupled few-mode fibers presenting different refractive index profiles. The results are compared with those obtained by more sophisticated experiments based on the analysis of the angular distribution of light scattering.

## 1. Introduction

Since 2010, few mode fibers (FMF) have generated a lot of interest as one of the alternatives to meet the need for data transmission with increased capacity in fiber networks. Recent developments in FMF have demonstrated the expected capacity gain per fiber compared to the best single-mode fiber (SMF) performances, thanks to the implementation of mode division multiplexing (MDM) [1]. However, among other parameters, the differential mode attenuation (DMA) that these fibers face must be kept below 0.01 dB/km in order to allow the capacity gain [2]. In SMF, the losses are now well understood and controlled while, in FMF, the situation is more complex because each mode undergoes the waveguide differently due to its unique intensity distribution. As a result, each mode – especially the linearly polarized (LP) modes commonly encountered in optical fibers – has a specific light scattering signature, with this mechanism contributing to the majority of optical losses and part of the DMA at telecommunications wavelengths [3]. In this work, attention is focused on weakly-coupled FMF, where the modes propagate with low coupling and thus low crosstalk (XT) thanks to a large effective index difference  $|\Delta n_{eff}|$  between them. Bidirectional optical time-domain reflectometry (OTDR) is applied in order to be able to easily access to the backscattering properties of the different LP modes in different fibers spliced together. The basics of bidirectional OTDR are first revisited and then validated using three different SMF. Then, the technique is used to

compare the Rayleigh scattering coefficients of the same LP modes of two FMF with different refractive index profiles (RIP).

## 2. Optical time domain reflectometry

As is well-known, OTDR technique consists in injecting, at  $z = 0$ , a light pulse of power  $P_0^{v\mu}$  and time duration  $\tau$  on a mode LP $_{v\mu}^{v\mu}$  that has an effective area  $S_{eff}^{v\mu}$  and propagates with a group velocity  $v_g^{v\mu}$ . During propagation, the pulse undergoes Rayleigh scattering (coefficient  $\bar{\alpha}_R^{v\mu}$ ) at each position  $z$ . The backscattered power  $B^{v\mu}$  is notably found in the same counter-propagating mode whose intensity is detected at the fiber input as a function of time and then space using the formula  $2z = v_g^{v\mu}t$ . Therefore, the optical power scattered by a mode and captured by the same counter-propagating mode, can be expressed as follows a function of the fiber length [4–7]:

$$P^{v\mu}(z) = P_0^{v\mu} \frac{\tau v_g^{v\mu}}{2} \bar{\alpha}_R^{v\mu} B^{v\mu} e^{-2\alpha^{v\mu}z} \quad (1)$$

where  $\alpha^{v\mu}$  is the total attenuation of the mode and  $\bar{\alpha}_R^{v\mu}$  is the radial average of the local attenuation coefficient of Rayleigh scattering for a guided mode of the fiber. Using the overall capture fraction,  $B^{v\mu}$ , developed in ref. [8] the backscattering factor can be defined as [9]:

$$\eta^{v\mu} = \frac{\tau v_g^{v\mu}}{2} \frac{3\pi}{2n^2 k_0^2} \frac{\bar{\alpha}_R^{v\mu}}{S_{eff}^{v\mu}} \quad (2)$$

\* Corresponding author.

E-mail address: [maroun.bsaibes@univ-lille.fr](mailto:maroun.bsaibes@univ-lille.fr) (M. Bsaibes).

Where  $n$  is the refractive index of the core and  $k_0$  is the wavevector in vacuum.  $S_{\text{eff}}^{\nu\mu}$  is defined as:

$$S_{\text{eff}}^{\nu\mu} = \frac{\left( \iint_A \Psi_{\nu\mu}^2(r, \phi) dA \right)^2}{\iint_A \Psi_{\nu\mu}^4(r, \phi) dA} \quad (3)$$

Where  $\Psi_{\nu\mu}$  represents the mode field distribution,  $A$  denotes the cross-sectional area, and  $r$  and  $\phi$  correspond to the radial and azimuthal coordinates, respectively.

$\tilde{\alpha}_R^{\nu\mu}$  is the radial average of the local attenuation coefficient of the Rayleigh scattering weighted by the radial extension to the power of four:

$$\tilde{\alpha}_R^{\nu\mu} = \frac{\iint_A \alpha_R(r, \phi) \Psi_{\nu\mu}^4(r, \phi) dA}{\iint_A \Psi_{\nu\mu}^4(r, \phi) dA} \quad (4)$$

Substituting Eq. (2) in Eq. (1) gives:

$$P^{\nu\mu}(z) = P_0^{\nu\mu} \eta^{\nu\mu} e^{-2\alpha^{\nu\mu} z} \quad (5)$$

Then, the ratio of Rayleigh scattering coefficients of the same mode propagating in two different fibers  $\mathbb{A}$  and  $\mathbb{B}$  is then given by:

$$\frac{\tilde{\alpha}_{R,\mathbb{A}}^{\nu\mu}}{\tilde{\alpha}_{R,\mathbb{B}}^{\nu\mu}} = \frac{S_{\text{eff},\mathbb{A}}^{\nu\mu} v_{g,\mathbb{B}}^{\nu\mu} \eta_{\mathbb{A}}^{\nu\mu} n_{\mathbb{A}}^2}{S_{\text{eff},\mathbb{B}}^{\nu\mu} v_{g,\mathbb{A}}^{\nu\mu} \eta_{\mathbb{B}}^{\nu\mu} n_{\mathbb{B}}^2} \quad (6)$$

The aim of the next section is to evaluate how bidirectional OTDR can give access to the ratio  $\eta_{\mathbb{A}}^{\nu\mu} / \eta_{\mathbb{B}}^{\nu\mu}$ .

### 3. Bidirectional OTDR measurement

In 1979, P. Di Vita et al. theoretically proposed the concept of using OTDR for separating power fading contributions caused by irregularities in the optical fibers [10]. This concept was demonstrated experimentally in 1982 and the local attenuation coefficient and the local backscattering factor have hence been measured separately [11]. Since then, multiple studies have reported the comparison of the Rayleigh scattering coefficients of two SMF spliced together [9,12,13]. It appears that a bidirectional measurement is sufficient to extract the backscattering factor of a mode for a given fiber. This consists of performing measurements on both sides of the fiber by injecting a pulse power  $P_0^{\nu\mu}$  through one end and capturing the backscattered power  $P^{\nu\mu}(z)$  from the same input and doing the same at the other end with an input power  $P_1^{\nu\mu}$  so that the collected power is  $P^{\nu\mu}(L-z)$ . Then, by summing bidirectional traces  $S^{\nu\mu}(z) = 5\log_{10}(P^{\nu\mu}(z))$  and  $S^{\nu\mu}(L-z) = 5\log_{10}(P^{\nu\mu}(L-z))$  using Eq. (5), the attenuation coefficient  $-2\alpha^{\nu\mu}$  can be removed and the following quantity can be deduced:

$$I^{\nu\mu} = S^{\nu\mu}(z) + S^{\nu\mu}(L-z) = 5\log_{10}(P_0^{\nu\mu} P_1^{\nu\mu}) + 10\log_{10}(\eta^{\nu\mu}(z)) \quad (7)$$

In practice,  $P_0^{\nu\mu}$  and  $P_1^{\nu\mu}$  are unknown which makes it impossible to extract  $\eta^{\nu\mu}(z)$ . So as to access this quantity, a measurement based on the splicing of two fibers is then used. Let's consider two fibers  $\mathbb{A}$  and  $\mathbb{B}$  spliced at position  $z_0$ . Both fibers are supposed to possess their own attenuation coefficient ( $\alpha_{\mathbb{A}}^{\nu\mu}$  and  $\alpha_{\mathbb{B}}^{\nu\mu}$  respectively) and their own backscattering factor ( $\eta_{\mathbb{A}}^{\nu\mu}$  and  $\eta_{\mathbb{B}}^{\nu\mu}$  respectively). Performing bidirectional measurements by exciting the same mode, the bidirectional traces will present a discontinuity at position  $z_0$ . This is due to the fact that the mode undergoes, among other, a different attenuation coefficient and a different refractive index when it passes from one fiber to the other [12]. To return to the idea of the sum of the bidirectional traces, the sum in this case will also present a discontinuity at the position  $z_0$ . This discontinuity corresponds to the difference of the backscattering factors between the two fibers by exciting the same mode and is calculated using Eq. (7) as:

$$D^{\nu\mu} = I_{\mathbb{A}}^{\nu\mu} - I_{\mathbb{B}}^{\nu\mu} = 10\log_{10}\left(\frac{\eta_{\mathbb{A}}^{\nu\mu}}{\eta_{\mathbb{B}}^{\nu\mu}}\right) \Rightarrow \frac{\eta_{\mathbb{A}}^{\nu\mu}}{\eta_{\mathbb{B}}^{\nu\mu}} = 10^{\frac{D^{\nu\mu}}{10}} \quad (8)$$

**Table 1**

SMF fibers used to validate the bidirectional OTDR method.

	Name	Supplier	Core type
SMF1	G654	Sumitomo	Silica [14]
SMF2	G652	Prysmian	Ge-doped
SMF3	G654	Prysmian	Ge-doped

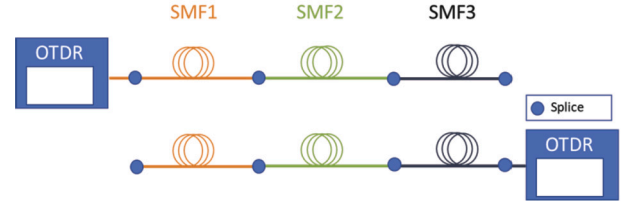


**Fig. 1.** Setup of bidirectional OTDR measurement for three SMF spliced together.

It can be noted that another important parameter can be extracted using bidirectional OTDR measurement which is the splice loss. To do so, it is necessary to perform the subtraction of the bidirectional OTDR measurement as follows:

$$Y^{\nu\mu} = S^{\nu\mu}(z) - S^{\nu\mu}(L-z) = 5\log_{10}\left(\frac{P_0^{\nu\mu}}{P_1^{\nu\mu}}\right) - 2(2\alpha^{\nu\mu}z + \alpha_{\text{splice}}^{\nu\mu}) \quad (9)$$

Where  $\alpha_{\text{splice}}^{\nu\mu}$  is the splice loss.

### 4. Experimental validation

In order to validate our experimental implementation of the theoretical model presented in the previous section, we first applied the bidirectional OTDR method to three different SMF presented in Table 1. Using a commercial OTDR system (8000 series OTDR, Photon Kinetics), bidirectional traces were recorded at three wavelengths (1410 nm, 1550 nm and 1625 nm) using the experimental setup described in Fig. 1. This first experiment is similar to the one conducted by Guenot et al. to put in evidence an extra-loss mechanism which is added to Rayleigh scattering [9].

An example of bidirectional traces at 1410 nm is reported in Fig. 2(a). At each splice between fibers, a discontinuity is observed and contains information about the splice losses and the change of fiber characteristics (attenuation coefficients, refractive index change, mode area...). In order to extract the ratio of backscattering factors between the three fibers, the bidirectional traces are summed together (Eq. (7)) as shown in Fig. 2(b). The curve in Fig. 2(b) presents a discontinuity, noted  $D^{\nu\mu}$ , at each fiber junction. On both sides of each discontinuity, horizontal lines with some fluctuations represent the longitudinal fluctuation of the backscattering coefficient for each fiber. By fitting the horizontal lines and applying Eq. (8), the ratio of the backscattering factor between two fibers can be extracted (see Table 2). It clearly appears that the backscattering factors are different for the three fibers and are wavelength-dependent.

Using the refractive index profile of each fiber, the group index and the effective area of the fundamental mode can be calculated. Then, the ratio of Rayleigh coefficients can be extracted at each wavelength, using Eq. (6). Table 2 shows a good agreement between the ratios at different wavelengths. SMF1 presents smaller Rayleigh coefficient than SMF2 and SMF3 since the ratios of Rayleigh coefficients (0.80 and 0.83, respectively) are smaller than the unity. This was expected because SMF1 is a silica-core fiber. On the other hand, SMF2 presents a higher Rayleigh coefficient than SMF3 (1.04), the ratio being larger than the unity.

The extraction of the ratio of Rayleigh coefficients between different fibers has been validated at three different wavelengths. This approach

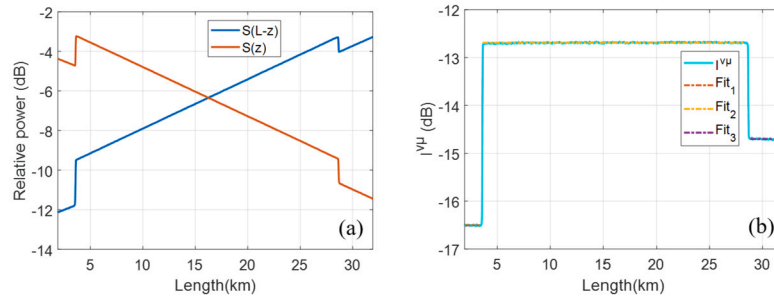


Fig. 2. Example at 1410 nm of (a) OTRD bidirectional traces, (b) sum of bidirectional traces for three SMF spliced together.

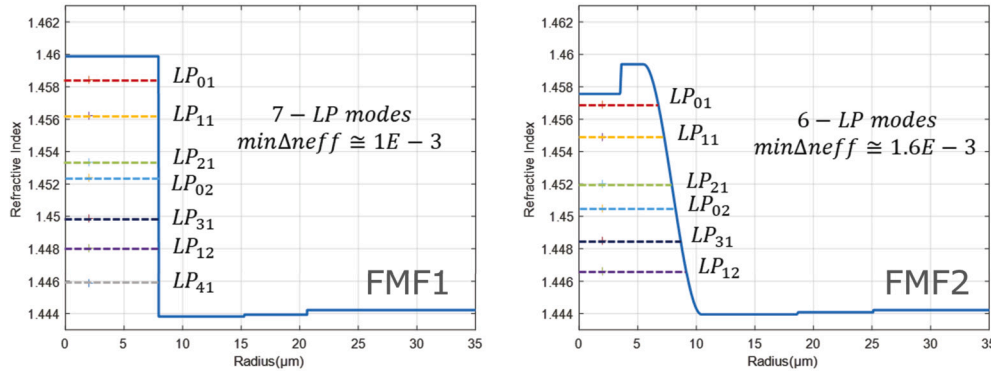


Fig. 3. Refractive index profiles at 1550 nm of the two FMF under test: FMF1 with a step-index RIP, FMF2 with a trapezoidal-index RIP.

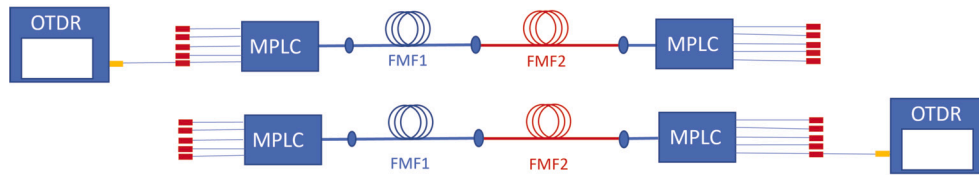


Fig. 4. Experimental setup of a bidirectional OTRD measurement for FMF.

Table 2

Backscattering factor difference and the ratio of Rayleigh scattering coefficients between the different fibers (SMF1, SMF2 and SMF3) at three different wavelengths (1410 nm, 1550 nm and 1625 nm).

Wavelength (nm)	1410	1550	1625
$D_{SMF1/SMF2}^{01}$	-3.81	-3.59	-3.46
$D_{SMF2/SMF3}^{01}$	2.01	1.81	1.70
$D_{SMF1/SMF3}^{01}$	-1.80	-1.77	-1.76
$\tilde{\alpha}_{R,SMF1}^{01} / \tilde{\alpha}_{R,SMF2}^{01}$	0.80	0.80	0.80
$\tilde{\alpha}_{R,SMF1}^{01} / \tilde{\alpha}_{R,SMF3}^{01}$	0.83	0.83	0.83
$\tilde{\alpha}_{R,SMF2}^{01} / \tilde{\alpha}_{R,SMF3}^{01}$	1.03	1.04	1.04

Table 3

Overlap integral between the modes of FMF1 and FMF2 at 1550 nm.

FMF2\FMF1	LP <sub>01</sub>	LP <sub>11</sub>	LP <sub>21</sub>	LP <sub>02</sub>	LP <sub>31</sub>	LP <sub>12</sub>
LP <sub>01</sub>	99.57%	0.00%	0.00%	0.28%	0.00%	0.00%
LP <sub>11</sub>	0.00%	99.85%	0.00%	0.00%	0.00%	0.00%
LP <sub>21</sub>	0.00%	0.00%	99.72%	0.00%	0.00%	0.00%
LP <sub>02</sub>	0.28%	0.00%	0.00%	99.11%	0.00%	0.00%
LP <sub>31</sub>	0.00%	0.00%	0.00%	0.00%	99.43%	0.00%
LP <sub>12</sub>	0.00%	0.00%	0.00%	0.00%	0.00%	96.36%

- the modes of different groups do not have to be coupled together as is the case of a graded index fiber, in order to prevent the backscattered light to contain different characteristics of the coupled modes that are complex to separate.

In this study, two weakly-coupled FMF with different index profiles will be investigated (Fig. 3):

- FMF1 is a step-index fiber and support 7-LP modes with minimum  $|\Delta n_{eff}|$  ( $min|\Delta n_{eff}|$ ) between modes of  $1 \times 10^{-3}$ . (In the following, 6-LP modes are evaluated due to the limitation of the multiplexer.)
- FMF2 has a trapezoidal index profile and supports 6-LP modes with a depressed index region in the core so that  $min|\Delta n_{eff}| = 1.6 \times 10^{-3}$  [15].

The overlap integrals between the modes of the two fibers have been calculated and the values are reported in Table 3. It can be noted that the diagonal values are very large while the off-diagonal ones are small

has also been experimentally validated with low and high attenuation splices (not shown here). In the following, we will be focusing on the transposition of this method to FMF.

### 5. Experimental measurement on FMF

Our goal is to compare the Rayleigh scattering coefficients of different modes of different FMF. Compared to the case of SMF, the situation is a bit different at the splice point for FMF:

- the overlap integral between the modes (same LP<sub>vμ</sub> mode) of the two fibers is very important. In the case of a bad overlap between modes, XT can be generated and the backscattered light contains some information that can be very difficult to differentiate.

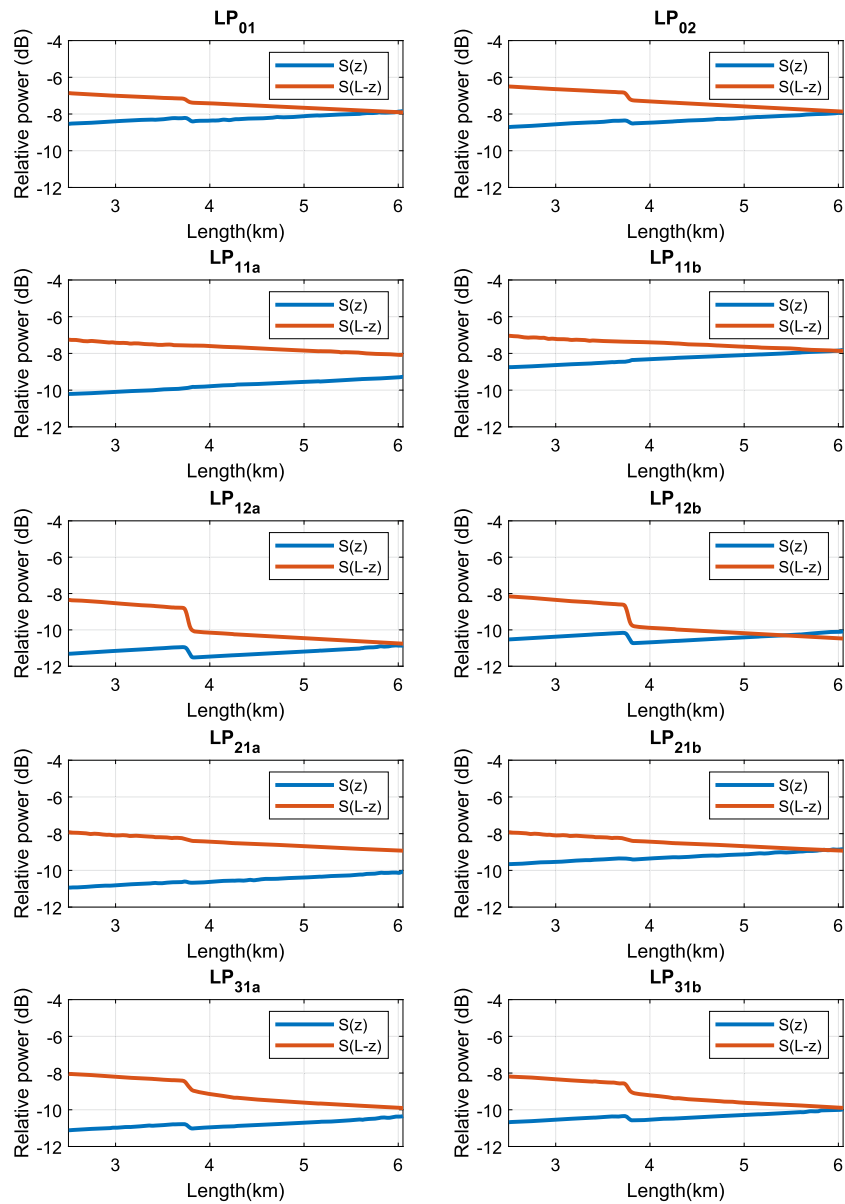


Fig. 5. Bidirectional OTDR traces at 1550 nm when FMF1 and FMF2 are spliced together.

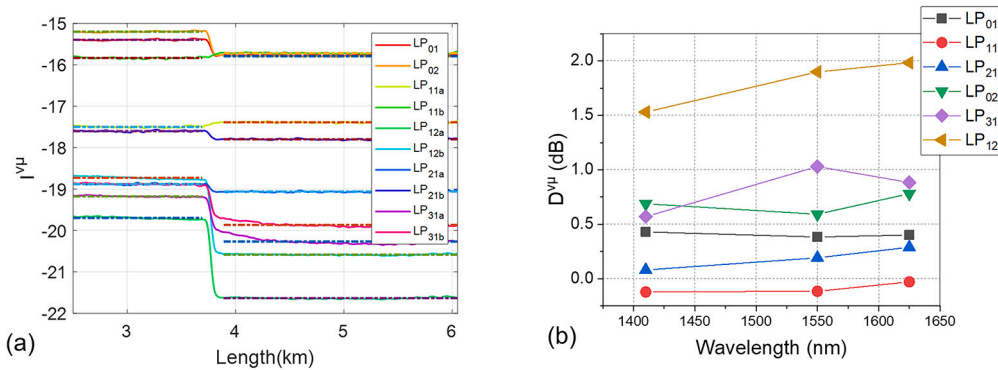


Fig. 6. (a) Sum of bidirectional traces at 1550 nm for the different modes, and (b) ratio of the backscattering factor between FMF1 and FMF2.

enough that the fibers can be spliced with an expected XT value of less than -20 dB.

Two spans of FMF1 and FMF2 were spliced together. Using multiplexers (MPLC from Cailabs) on both sides and the OTDR system

already used with SMF, bidirectional traces are recorded at three wavelengths (1410 nm, 1550 nm, and 1625 nm) by successively exciting the different modes as shown in Fig. 4. An example of bidirectional traces recorded by exciting each mode at 1550 nm is represented in Fig. 5.

**Table 4**

Effective area and group index of the different modes of FMF1 and FMF2 respectively at three different wavelengths (1410 nm, 1550 nm and 1625 nm).

FMF1 Wavelength (nm)	$S_{eff}$			$n_g$		
	1410	1550	1625	1410	1550	1625
LP <sub>01</sub>	122.5	125.6	127.3	1.4782	1.4789	1.4794
LP <sub>11</sub>	112.2	115.6	117.6	1.4796	1.4805	1.4811
LP <sub>21</sub>	99.1	103.8	106.8	1.4819	1.4830	1.4837
LP <sub>02</sub>	116.4	121.0	123.7	1.4814	1.4825	1.4832
LP <sub>31</sub>	116.7	123.2	127.3	1.4834	1.4846	1.4854
LP <sub>12</sub>	99.2	108.9	116.6	1.4840	1.4848	1.4851

FMF2 Wavelength (nm)	$S_{eff}$			$n_g$		
	1410	1550	1625	1410	1550	1625
LP <sub>01</sub>	135.6	137.6	138.8	1.4767	1.4774	1.4779
LP <sub>11</sub>	106.6	111.7	114.6	1.4783	1.4792	1.4798
LP <sub>21</sub>	92.2	102.5	108.6	1.4794	1.4802	1.4808
LP <sub>02</sub>	113.7	121.4	125.8	1.4800	1.4809	1.4816
LP <sub>31</sub>	122.3	133.8	141.0	1.4815	1.4824	1.4829
LP <sub>12</sub>	125.9	149.2	168.2	1.4798	1.4798	1.4796

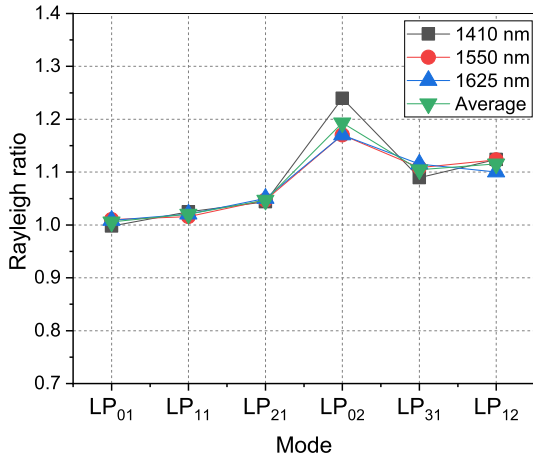


Fig. 7. Modal ratios of Rayleigh scattering coefficients between FMF1 and FMF2.

As before, the bidirectional traces obtained for each mode were summed so as to extract the ratio of backscattering factor as shown in Fig. 6(a). Therefore, the amplitude of the discontinuity  $D^{v\mu}$  for each mode is calculated using Eq. (8). Note that the degenerated modes (odd and even modes) are strongly coupled: the ratio of backscattered factor has then been averaged such as:  $D^{v\mu} = (D_o^{v\mu} + D_e^{v\mu})/2$ . Fig. 6(b) shows that the discontinuity is mode and wavelength dependent.

The effective area and group index of the different modes in each fiber are calculated using the RIP measured on fibers (see Table 4). According to Eq. (6), the ratio of the Rayleigh coefficients for the same mode can be extracted at each wavelength. Fig. 7 shows a good agreement between the ratios at different wavelengths and also shows that ratios are larger than unity, which means that the step-index fiber presents, for all the modes, a higher Rayleigh coefficient than the trapezoidal index fiber.

Finally, the bidirectional OTDR measurement of the different modes has been subtracted as shown in Fig. 8(a) so as to extract the splice at-

tenuation of each mode. The results are presented in Fig. 8(b). Note that the splice loss of the degenerated modes has been averaged. This last figure shows that, as expected, the splice loss depends on the mode. More interestingly, it shows that LP<sub>12</sub> mode presents the highest splice loss, which was expected because the overlap integral of this mode between the two fibers is only about 96%.

**6. Comparison with the results of angular distribution of the scattered intensity method**

To push further our study and to have a point of comparison of different methods, the results obtained here have been compared to those obtained using the measurement of the angular distribution of the scattered intensity of each mode of FMF1 and FMF2. This approach, described in ref. [3], not only allows to quantify the Rayleigh coefficients of the different modes of different fibers but also permits to put in evidence and quantify the contribution of extra-loss mechanism known as small-angle light scattering (SALS). Fig. 9 shows that the Rayleigh coefficients of FMF1 are higher than those of FMF2, which can be explained by the larger core index of FMF1 compared to FMF2.

In order to compare these results to those of bidirectional OTDR, the ratio  $\tilde{\alpha}_{R,FMF1}^{v\mu} / \tilde{\alpha}_{R,FMF2}^{v\mu}$  (the overlap between the intensity distribution of the mode and Rayleigh coefficient distribution, which corresponds to what is measured using the recording of the angular distribution of the scattered light) has first to be theoretically compared to the ratio  $\tilde{\alpha}_{R,FMF1}^{v\mu} / \tilde{\alpha}_{R,FMF2}^{v\mu}$  (Eq. (4) which corresponds to what is measured using bidirectional OTDR method). Using ref. [16], the radial dependence of the Rayleigh scattering coefficients can be obtained and the two ratios can be calculated for each mode. The results obtained are presented in Fig. 10(a) that shows that the two values are in good agreement. Consequently, these ratios can be compared experimentally.

Using the Rayleigh scattering coefficients of the different modes of the two fibers extracted from the angular scattered intensity distribution method, the ratio of the Rayleigh scattering coefficients can be calculated and thus can be compared to that of the bidirectional OTDR method. Fig. 10(b) shows good agreement between the two methods with however a larger difference for the LP<sub>02</sub> mode. The proposed bidirectional OTDR method thus appears as a simple and efficient method

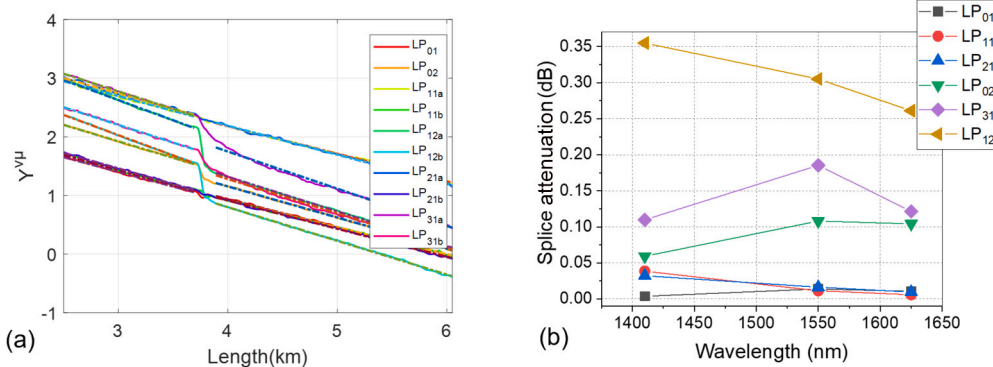


Fig. 8. (a) Subtraction of bidirectional traces at 1550 nm for the different modes, (b) and the splice attenuation, by exciting the different modes as a function of wavelength.

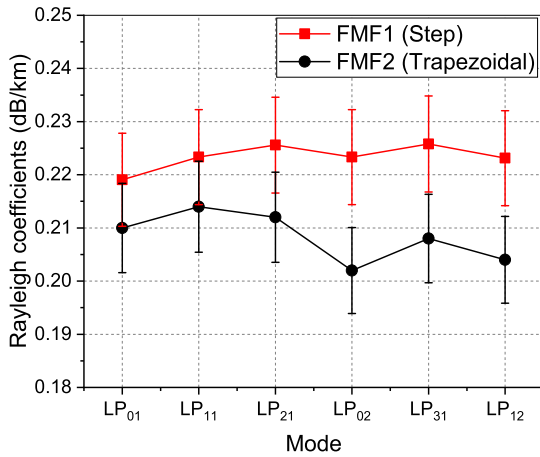


Fig. 9. Modal Rayleigh scattering coefficients at 1550 nm of fibers E and B obtained using the angular distribution of the scattered intensity method presented in ref. [3].

to compare the Rayleigh scattering coefficients of different modes of two FMF. The OTDR bidirectional measurement demonstrates superior precision compared to the angular distribution method, with an uncertainty level of approximately 2%. In contrast, the angular distribution method yields a higher uncertainty when determining the Rayleigh ratios of about 8% due to the measurement difficulties when measuring laterally the light scattered from the fibers. These uncertainty values are determined by performing a thorough analysis of 10 consecutive measurements.

The proposed method offers a straightforward and easily implementable tool for comparing and optimizing FMFs. It goes beyond by providing the capability to access individual modal properties, including the individual Rayleigh scattering coefficients and mode effective areas. This access to essential modal properties empowers researchers and engineers, enabling them to gain valuable insights into the performance and characteristics of various FMFs. Consequently, this valuable information facilitates the design and development of more efficient and tailored optical communication systems and fiber optic sensing applications.

### 7. Conclusion

In this paper, the theoretical principle of OTDR has been discussed to define the backscattering factor as a function of the Rayleigh scattering coefficient and the effective area of a guided mode. The principle of bidirectional OTDR has been developed showing that by splicing two fibers, it is possible to extract the ratio of backscattering factors by summing the bidirectional traces. From this later ratio, it is possible to compare the ratio of the Rayleigh scattering coefficients by excit-

ing the same mode. In addition, it has been shown that by subtracting the bidirectional traces, one can extract the attenuation of the modes propagating in the different fibers and the splice loss. This theoretical approach was validated by splicing three SMF and comparing them at three different wavelengths. Furthermore, it has been tested that even with high splice attenuation, it is possible to extract the Rayleigh scattering ratio between two fibers. After the validation of the principle, bidirectional OTDR measurements on two FMF have been recorded and the mode-dependent ratios of the Rayleigh scattering coefficients have been deduced by exciting the different modes. Finally, the results of the bidirectional OTDR method have been compared to those of the angular distribution of the scattered intensity method and a good agreement has been found. It is concluded that bidirectional OTDR is a simple and effective method for comparing Rayleigh scattering coefficients of different modes in two FMFs, under the condition that the two fibers have a good overlap between their modes.

### CRediT authorship contribution statement

**Maroun Bsaibes:** Conceptualization, Methodology, Validation, Formal analysis, Investigation, Data curation, Writing – original draft, Writing – review & editing, Visualization. **Yves Quiquempois:** Conceptualization, Methodology, Validation, Formal analysis, Investigation, Writing – review & editing, Visualization, Supervision. **Marianne Bigot:** Resources, Writing – review & editing. **Pierre Sillard:** Resources, Writing – review & editing. **Maxime Droques:** Resources. **Masaaki Hirano:** Resources. **Laurent Bigot:** Conceptualization, Methodology, Validation, Formal analysis, Investigation, Writing – review & editing, Visualization, Supervision, Project administration, Funding acquisition.

### Declaration of competing interest

The authors declare that they have no known competing financial interests or personal relationships that could have appeared to influence the work reported in this paper.

### Data availability

Data underlying the results presented in this paper are not publicly available at this time but may be obtained from the authors upon reasonable request.

### Acknowledgements

This research was partially supported by the French Agence Nationale de la Recherche through the ANR MUPHTA project under Grant ANR-20-CE24-0016. Additionally, the Hauts-de-France Regional (HdF) Council provided support through the eLIFT project. The authors also acknowledge the financial assistance from the European Regional Development Fund (ERDF) and the I-SITE UNLE. Furthermore, this work

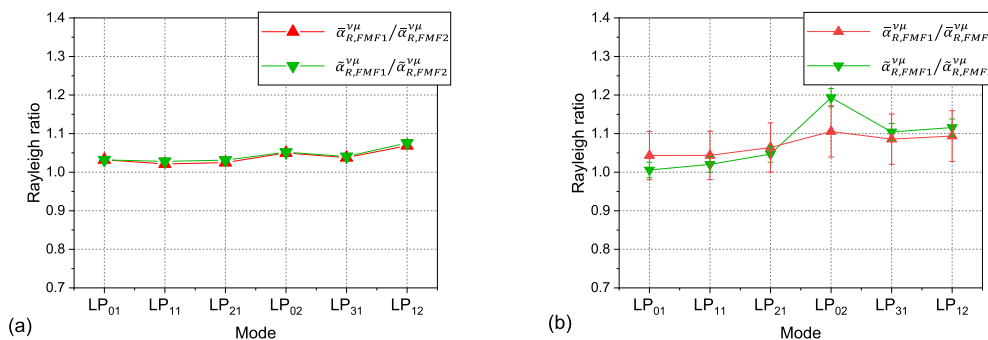


Fig. 10. (a) Theoretical and (b) experimental comparison between the ratios of Rayleigh scattering coefficients that can be extracted from the angular distribution of the scattered intensity (red) method and the bidirectional OTDR method (green).

was carried out within the framework of the Contrat de Plan Etat-Region (CPER WaveTech), which is supported by the Ministry of Higher Education and Research, the HdF Regional council, the Lille European Metropolis (MEL), the Institute of Physics of the French National Centre for Scientific Research (CNRS) and the ERDF. This work has been partially supported by IRCICA USR 3380 Univ. Lille – CNRS ([www.ircica.univ-lille.fr](http://www.ircica.univ-lille.fr)).

## References

- [1] Puttnam BJ, Rademacher G, Luís RS. Space-division multiplexing for optical fiber communications. *Optica* 2021;8(9):1186–203. <https://doi.org/10.1364/OPTICA.427631>. Publisher: Optica Publishing Group.
- [2] Sillard P, Bigot-Astruc M, Molin D. Few-mode fibers for mode-division-multiplexed systems. *J Lightwave Technol* 2014;32(16):2824–9. <https://doi.org/10.1109/JLT.2014.2312845>.
- [3] Bsaibes M, Quiquempois Y, Plus S, Masselot A, Labroille G, Bigot M, et al. Light scattering mechanisms in few-mode fibers. *J Lightwave Technol* 2022;40(10):3293–8. Publisher: IEEE.
- [4] Aoyama K, Nakagawa K, Itoh T. Optical time domain reflectometry in a single-mode fiber. *IEEE J Quantum Electron* 1981;17(6):862–8. <https://doi.org/10.1109/JQE.1981.1071237>.
- [5] Philen D, White I, Kuhl J, Mettler S. Single-mode fiber OTDR: experiment and theory. *IEEE Trans Microw Theory Tech* 1982;30(10):1487–96. <https://doi.org/10.1109/TMTT.1982.1131282>.
- [6] Brinkmeyer E. Analysis of the backscattering method for single-mode optical fibers. *J Opt Soc Am* 1980;70(8):1010–2. <https://doi.org/10.1364/JOSA.70.001010>. Publisher: Optica Publishing Group.
- [7] Hartog A, Gold M. On the theory of backscattering in single-mode optical fibers. *J Lightwave Technol* 1984;2(2):76–82. <https://doi.org/10.1109/JLT.1984.1073598>.
- [8] Bisyarin MA, Kotov OI, Hartog AH, Liokumovich LB, Ushakov NA. Rayleigh backscattered radiation produced by an arbitrary incident mode in multimode optical fibers. *Appl Opt* 2018;57(22):6534. <https://doi.org/10.1364/AO.57.006534>.
- [9] Guenot P, Nouchi P, Poumellec O, Mercereau B. Investigation of single-mode optical fiber loss properties by OTDR measurements. In: *Proceedings of forty-fifth IWCS; International wire and cable symposium; 1996*. p. 679–88.
- [10] di Vita P, Rossi U. The backscattering technique – its field of applicability in fibre diagnostics and attenuation measurements. *Opt Quantum Electron* 1980;12:17–22.
- [11] Gold MP, Hartog AH. Determination of structural parameter variations in single-mode optical fibres by time-domain reflectometry. *Electron Lett* 1982;18(12):489–90. <https://doi.org/10.1049/el:19820332>.
- [12] Fermann M, Poole S, Payne D, Martinez F. Comparative measurement of Rayleigh scattering in single-mode optical fibers based on an OTDR technique. *J Lightwave Technol* 1988;6(4):545–51. <https://doi.org/10.1109/50.4036>.
- [13] Tsujikawa K, Tajima K, Ieda K, Nakajima K, Kurokawa K, Shiraki K, et al. Evaluation of Rayleigh scattering loss in photonic crystal fibers by using bi-directional OTDR measurement. In: *OFC/NFOEC 2007 – 2007 conference on optical fiber communication and the national fiber optic engineers conference; 2007*. p. 1–3.
- [14] Available from: <https://global-sei.com/ftx/optical-fibers/z-fiber/>; 2023.
- [15] Bigot-Astruc M, Trinel JB, Maerten H, van Stralen M, Milicevic I, Bigot L, et al. Weakly-coupled 6-LP-mode fiber with low differential mode attenuation. In: *2019 optical fiber communications conference and exhibition; 2019*. p. 1–3.
- [16] Ohashi M, Shiraki K, Tajima K. Optical loss property of silica-based single-mode fibers. *J Lightwave Technol* 1992;10(5):539–43. <https://doi.org/10.1109/50.136085>.